Supplementary data

Table S1: Clinical characteristics of discovery and validation cohorts.

Discovery Cohort (FFPE)					
Sample Type	**Sample ID**	**Age (yrs.)**	**Sample types**	**PSA**	**Gleason score**
BPH* (N = 8)	22	72	Biopsy	27.32	NA
	74	56	Biopsy	12.3	NA
	75	61	Biopsy	2.92	NA
	81	55	Biopsy	4.9	NA
	102	77	Biopsy	8	NA
	103	80	Biopsy	51.81	NA
	106	65	Biopsy	7.84	NA
	119	60	Biopsy	16.97	NA
PCa# (N = 8)	24	45	Biopsy	149	4+4=8/10
	70	73	Biopsy	78.5	3+3=6/10
	93	62	Biopsy	57.08	3+3=6/10
	131	71	Biopsy	68.4	4+3=7/10
	143	50	Biopsy	162	3+4=7/10
	180	78	Biopsy	1777	3+4=7/10
	187	65	Biopsy	40.2	3+4=7/10
	324	63	Biopsy	4.46	3+4=7/10
Validation Cohort (Freshly frozen)					
Sample Type	**Sample ID**	**Age (yrs.)**	**Sample types**	**PSA**	**Gleason score**
BPH* (N = 8)	B1	76	Biopsy	21.38	NA
	B3	67	Biopsy	25	NA
	B4	68	Biopsy	6.13	NA
	B6	70	Biopsy	13.6	NA
	B7	70	Biopsy	33.7	NA
	B8	69	Biopsy	7.81	NA
	B9	65	Biopsy	6.52	NA
	B10	80	Biopsy	6.2	NA
PCa# (N = 8)	PC1	83	Biopsy	38.6	5+4=9/10
	PC2	54	Biopsy	88	5+5=10/10
	PC3	67	Biopsy	66.7	5+4=9/10
	PC4	62	Biopsy	45	5+4=9/10
	PC5	60	Biopsy	331.27	4+5=9/10
	PC6	79	Biopsy	54.17	5+4=9/10
	PC7	77	Biopsy	184	5+5=10/10
	PC10	65	Biopsy	102	5+3=8/10

* BPH: benign prostatic hyperplasia; #PCa: prostate cancer

Table S2. Previously published datasets used in this study.

Accession ID	Experiment	Target	Cell line/tissue samples
GSE66039	ChIP-Seq	5-mC	LNCaP
GSE83860		AR	LNCaP
GSE117430		AR	LNCaP
GSE47987		AR	DU145
GSE43253		RNA Pol II	LNCaP
GSE114737		H3K27ac	LNCaP
GSE94013		BRD4	22RV1
GSE130408		H3K27ac	Prostate tissue samples
GSE120742			
GSE188173			
GSE55062		AR	VCaP
		RNA Pol II	
GSE83653		AR	VCaP
GSE70079		AR	Prostate tissue samples
GSE56086		FOXA1	VCaP
GSE37345		FOXA1	LNCaP
GSE146886		RNA Pol II	22RV1
GSE57498		H3K27ac	PrEC
GSE105290			RWPE1
GSE229871			VCaP
GSE205885	ATAC-Seq		LNCaP
GSE181294	ScRNA-Seq		Prostate tissue samples
GSE223024	RNA-Seq		LNCaP
			VCaP
GSE80741			22RV1
GSE71797			VCaP
GSE95413			VCaP
GSE139230			LNCaP
GSE250422			LNCaP
GSE184168			C4-2R
GSE80609			Prostate tissue samples
GSE119757			LNCaP
GSE193127			VCaP
GSE25346	Micro Array		LNCaP
GSE63196			DU145
			LNCaP
			22RV1
GSE38240	450K Methylation EPIC Array		Prostate tissue samples
GSE112047			
GSE62053			LNCaP
GSE66872			DU145

GSE54758		
GSE86832	Bisulfite Sequencing	LNCaP
GSE42790		DU145

Table S3: Gene expressions in different prostate cell lines from DepMap portal.*

Sl No	DepMap Id	Cell Lines	Lineage	AR	DUOX1	DNMT1	DNMT3A	DNMT3B	BRD4
1	ACH-000162 7	P4E6	Immortalized Epithelial Cells, Prostate	0	4.849409	5.81556	3.178413	2.781228	3.770797
2	ACH-000170	PRECLH	Immortalized Epithelial Cells, Prostate	0.021505	3.740021	7.021091	3.999928	3.22077	5.433888
3	ACH-001648	SHMAC4	Immortalized Epithelial Cells, Prostate	0	6.133463	4.687369	3.296983	1.587658	3.959844
4	ACH-001649	SHMAC5	Immortalized Epithelial Cells, Prostate	0.007607	6.179169	4.677948	3.39282	1.002292	3.952594
5	ACH-001422	WPE1NA22	Immortalized Epithelial Cells, Prostate	0	4.504747	5.274236	2.176904	0.463538	3.675172
6	ACH-001453	BPH1	Hyperplasia, Prostate	0.0039	5.908001	5.922971	2.197881	2.133748	4.232553
7	ACH-000090	PC3	Prostate Adenocarcinoma	0.010584	0.606528	6.458759	2.710874	1.286627	3.2946
8	ACH-000979	DU145	Prostate Adenocarcinoma	0	1.962941	4.598502	1.515919	0.626829	2.201452
9	ACH-000977	LNCAPCLONEFGC	Prostate Adenocarcinoma	6.284431	1.223738	5.848595	4.13629	1.89815	4.708607
10	ACH-000115	VCAP	Prostate Adenocarcinoma	8.722278	0.227578	5.655767	4.56364	2.53859	5.299556
11	ACH-000952	MDAPCA2B	Prostate Adenocarcinoma	5.378213	0.478665	6.188312	3.342724	1.764057	4.891618
12	ACH-000956	22RV1	Prostate Adenocarcinoma	7.589449	0.539633	6.694574	4.166049	2.468959	4.505688

* RNA-Seq Log2 TPM+1 values were extracted from DepMap portal (https://depmap.org/portal/)

Table S4. Cell lines generated and used in this study.

Cell lines	Source	Identifier
LNCaP	Obtained from ATCC, USA	Cat No. CRL-1740
DU145	Obtained from ATCC, USA	Cat No. HTB-81
MyC-CaP	Obtained from ATCC, USA	Cat No. CRL-3255
Lenti-X 293T	Takara Bio Inc.	Cat No. 632180
LNCaP stably expressing DNMT3A Sh-RNA	This study	N/A
LNCaP stably expressing AR sgRNA#1	This study	N/A
LNCaP stably expressing AR sgRNA#2	This study	N/A
LNCaP stably expressing BRD4 sgRNA#1	This study	N/A
LNCaP stably expressing BRD4 sgRNA#2	This study	N/A
LNCaP stably expressing DUOX1-pLVX-TetOne-Puro lentiviral expression plasmid	This study	N/A
MyC-CaP stably expressing DUOX1-pLVX-TetOne-Puro lentiviral expression plasmid	This study	N/A
LNCaP stably expressing pLX302_FOXA1-V5 lentiviral expression plasmid	This study	N/A
LNCaP stably expressing FOXA1 sgRNA#1	This study	N/A

Table S5. Antibodies used in this study.

Antibodies		
Anti-DUOX1 (H-9; Mouse monoclonal)	Santa Cruz Biotechnology Inc.	Cat No. sc-393096
Anti-DUOX1 (Rabbit polyclonal)	Invitrogen/Thermo Fisher Scientific	Cat No. PA5-85452
Anti-DUOX1 (3B8D6; Mouse monoclonal)	Proteintech Group, Inc.	Cat No. 67226-1-Ig
Anti-Androgen Receptor ((D6F11) XP; Rabbit monoclonal) for ChIP-qPCR analysis	Cell Signaling Technology	Cat No. 5153S
Anti-Androgen Receptor (AR 441; Mouse monoclonal)	Invitrogen/Thermo Fisher Scientific	Cat No. MA5-13426
Anti-Androgen Receptor (AG17291; Rabbit polyclonal)	Proteintech Group, Inc.	Cat No. 22089-1-AP
Anti-GAPDH (6C5; Mouse monoclonal)	Santa Cruz Biotechnology Inc.	Cat No. sc32233
Anti-GAPDH (Rabbit polyclonal)	Company ABclonal, Inc	Cat No. AC027
Anti- β-Actin (Rabbit mononclonal)	Company ABclonal, Inc	Cat No. AC026
Anti-GFP (Rabbit polyclonal)	Abcam Ltd.	Cat No. ab290
Anti-Flag (M2; Mouse monoclonal)	Merck/Sigma-Aldrich	Cat No. F3165
Anti-C-Myc Epitope (Myc Tag Polyclonal Antibody)	Cloud-Clone Corp	Cat No. TAX162Ge01
Anti-DNMT1 (Rabbit polyclonal)	Invitrogen/Thermo Fisher Scientific Inc.	Cat No. PA5-30581
Anti-DNMT3A (EPR18455; Rabbit monoclonal)	Abcam Ltd.	Cat No. ab188470
Anti-DNMT3B (EPR3523 ; Rabbit monoclonal)	Abcam Ltd.	Cat No. ab79822
Anti-H3K27ac (Rabbit polyclonal) for ChIP-qPCR analysis	Abcam Ltd.	Cat No. ab4729
Anti-BRD4 (14H4L4; Rabbit monoclonal)	Invitrogen/Thermo Fisher Scientific Inc.	Cat No. PA5-30581
Anti V5-Tag (Mouse monoclonal)	Company ABclonal, Inc	Cat No. AE017
Anti-FOXA1 (Rabbit polyclonal)	Invitrogen/Thermo Fisher Scientific Inc.	Cat No. PA5-27157
Anti-PARP1 (Rabbit monoclonal)	ABclonal Inc.	Cat No. A19596
Anti-Cleaved PARP (F21-852; Mouse monoclonal)	BD Pharmingen	Cat No. 552596
Anti-Caspase 3 (31A1067; Mouse monoclonal)	Santa Cruz Biotechnology Inc.	Cat No. sc-56053
Caspase-9 Antibody (Rabbit polyclonal)	Cell Signaling Technology	Cat No. 9502S
Anti-GPX4 (Rabbit polyclonal)	Company ABclonal, Inc	Cat No. A1933
Anti-SOD2 (Rabbit polyclonal)	Company ABclonal, Inc	Cat No. A1340
Anti-c-Myc antibody (clone 9E10)	Sigma-Aldrich/ Merck	Cat No. MABE282
Anti-Desmoplakin (Rabbit polyclonal)	Cloud-Clone Corp	Cat No. PAC203Hu01

Anti-beta-catenin (E-5, Mouse monoclonal)	Santa Cruz Biotechnology Inc.	Cat No. sc-7963
Anti-Vimentin (Mouse monoclonal)	Cloud-Clone Corp	Cat No. MAB040Hu21
Anti-Snail Homolog 1 (Rabbit polyclonal)	Cloud-Clone Corp	Cat No. PAK089Hu01
Rabbit IgG Isotype control	Invitrogen/Thermo Fisher Scientific Inc.	Cat No. 02-6102
Goat anti-Mouse IgG (H+L) Secondary Antibody, DyLight 680	Invitrogen/Thermo Fisher Scientific Inc.	Cat No. 35518
Goat anti-Mouse IgG (H+L) Secondary Antibody, DyLight 800 4X PEG	Invitrogen/Thermo Fisher Scientific Inc.	Cat No. SA5-35521
Goat anti-Rabbit IgG (H+L) Secondary Antibody, DyLight 800 4X PEG	Invitrogen/Thermo Fisher Scientific Inc.	Cat No. SA5-35571
Goat anti-Rabbit IgG (H+L) Secondary Antibody, DyLight™ 680	Invitrogen/Thermo Fisher Scientific Inc.	Cat No. 35568
Goat anti-Rabbit IgG, Alexa Fluor 488	Invitrogen/Thermo Fisher Scientific	Cat No. A-11008
Goat anti-Mouse IgG, Alexa Fluor 488	Invitrogen/Thermo Fisher Scientific	Cat No. A-11029
Goat anti-Rabbit IgG, Alexa Fluor 568	Invitrogen/Thermo Fisher Scientific	Cat No. A-11011
Goat anti-Mouse IgG, Alexa Fluor 568	Invitrogen/Thermo Fisher Scientific	Cat No. A-11004

Table S6. Oligo sequences used for qPCR, cloning of Sh-RNAs, sgRNAs, cDNAs, promoter regions and ChIP-qPCR.

Reagent or Resource	Source	Identifier
qRT-PCR oligonucleotides		
GAPDH qRT-PCR Fw- 5'- AATGAAGGGGTCATTGATGG -3' Rv- 5'- AAGGTGAAGGTCGGAGTCAA -3'	PMID: 38530845	N/A
B2M qRT-PCR Fw- 5'- GAGGCTATCCAGCGTACTCCA -3' Rv- 5'- CGGCAGGCATACTCATCTTTT -3'	PMID: 38530845	N/A
DUOX1 qRT-PCR Fw- 5'- AGCTCTGTGTCAAAGGGGTG -3' Rv- 5'- GAATCTCCTGGGGAGGGTCT-3'	This study	N/A
AR qRT-PCR Fw- 5'- GGTGAGCAGAGTGCCCTATC -3' Rv- 5'- GCAGTCTCCAAACGCATGTC -3'	This study	N/A
DNMT1 qRT-PCR Fw- 5'- ACAGCTTAACAGAAAAGGAATGTGT -3' Rv- 5'- TGACTTTAGCCAGGTAGCCCTC -3'	This study	N/A
DNMT3A qRT-PCR Fw- 5'- TGCCGGAACATTGAGGACAT -3' Rv- 5'- CCACAGCAGATGGTGCAGTA -3'	This study	N/A
DNMT3B qRT-PCR Fw- 5'- TCGTGCAGGCAGTAGGAAAT -3' Rv- 5'- GAAGCCATTTGTTCTCGGCTC -3'	This study	N/A
BRD4 qRT-PCR Fw- 5'- CAGTTGCGCCCAAAAAGGACC -3' Rv- 5'- CTGTCGCTGGATGACTTGGC -3'	This study	N/A
c-Myc qRT-PCR Fw- 5'-AGTGGAAAACCAGCAGCCTC -3' Rv- 5'-TTCTCCTCCTCGTCGCAGTA -3'	This study	N/A
TP53 qRT-PCR Fw- 5'- CTTCCCTGGATTGGCAGC -3' Rv- 5'- TTTCAGGAAGTAGTTTCCATAGGT -3'	PMID: 38530845	N/A
CDKN1A qRT-PCR Fw- 5'- ACAGCAGAGGAAGACCATGTG -3' Rv- 5'- CGTTTGGAGTGGTAGAAATCTGTC -3'	PMID: 38530845	N/A
UGT2B11 qRT-PCR Fw- 5'- GTGGGCATTCCATTGTTTTT -3' Rv- 5'- TTACTGGTTGATCATGTTGAATTC -3'	PMID: 21679149	N/A
UGT2B28 qRT-PCR Fw- 5'- ACCAGGATGGCTCTGAAGTG -3' Rv- 5'- ACACCAGCACCTTTCCACAA -3'	This study	N/A
CDH1 qRT-PCR Fw- 5'- TGCCCAGAAAATGAAAAAGG -3' Rv- 5'- GTGTATGTGGCAATGCGTTC -3'	This study	N/A
CTNNA1 qRT-PCR Fw- 5'- CTGGGAGGAGAGCTCATCA -3' Rv- 5'- TTTCACTGTTTGCACTACAGCATTC -3'	This study	N/A
CTNNB1 qRT-PCR	This study	N/A

Fw- 5’- TGTTCTCAGATTTCTGGTTGTT -3’ Rv- 5’- CACTTTCTGAGATACCAGCC -3’		
CLDN1 qRT-PCR Fw- 5’- CGATGAGGTGCAGAAGATGA -3’ Rv- 5’- CATTGACTGGGGTCATAGGG -3’	This study	N/A
SOX2 qRT-PCR Fw- 5’- GAGCTTTGCAGGAAGTTTGC -3’ Rv- 5’- GCAAGAAGCCTCTCCTTGAA -3’	PMID: 24681955	N/A
KLF4 qRT-PCR Fw- 5’- GCAGCCACCTGGCGAGTCTG -3’ Rv- 5’- CCGCCAGCGGTTATTCGGGG -3’	PMID: 24681955	N/A
NANOG qRT-PCR Fw- 5’- ACCTTGGCTGCCGTCTCTGG -3’ Rv- 5’- AGCAAAGCCTCCCAATCCCAAACA -3’	PMID: 24681955	N/A
Cloning oligonucleotides		
pLVX-TetOne-Puro-DUOX1 cloning primers Fw- 5’- AATGAGAATTCATGGGCTTCTGCCTGGCTC -3’ Rv- 5’- TATAAGGATCCCTAGAAGTTCTCATAATGGTGGG -3’	This study	N/A
sg-AR#1 Fw- 5’-CACCGGTCCCTGGCAGTCTCCAAAC-3’ Rv- 5’-AAACGTTTGGAGACTGCCAGGGACC-3’	This study	https://www.synthego.com/products/bioinformatics/crispr-design-tool
sg-AR#2 Fw- 5’-CACCGTTTCCAGTTTGGAGACTGCC -3’ Rv- 5’-AAACGGCAGTCTCCAAACTGGAAAC -3’	This study	https://www.synthego.com/products/bioinformatics/crispr-design-tool
sg-BRD4#1 Fw- 5’- CACCGTGGGATCACTAGCATGTCTG -3’ Rv- 5’- AAACCAGACATGCTAGTGATCCCAC -3’	This study	https://www.synthego.com/products/bioinformatics/crispr-design-tool
sg-BRD4#2 Fw- 5’- CACCGACTAGCATGTCTGCGGAGAG -3’ Rv- 5’- AAACCTCTCCGCAGACATGCTAGTC -3’	This study	https://www.synthego.com/products/bioinformatics/crispr-design-tool
sg-FOXA1#1 Fw- 5’- CACCGGGTTCATGGCGGCCGCGTAG -3’ Rv- 5’ - AAACCTACGCGGCCGCCATGAACCC -3’	This study	https://www.synthego.com/products/bioinformatics/crispr-design-tool
Sh-DNMT3A Fw-5’- TCGAGTGCTGTTGACAGTGAGCGActactacatcagcaagcgcaaTAGTGAAGCCACAGATGTAttgcgcttgctgatgtagtagGTGCCTACTGCCTCGGAA -3’ Rv-5’- CGCGTTCCGAGGCAGTAGGCACctactacatcagcaagcgcaaTACATCTGTGGCTTCACTAttgcgcttgctgatgtagtagTCGCTCACTGTCAACAGCAC -3’	This study	N/A
pGL3-DUOX1 AR pos cloning primers Fw- 5’- CCGAGCTCTTACGCGTCTGGCCAGCTGCCTGCAG -3’ Rv- 5’- TGCAGATCGCAGATCTCATGCTCATATCACTTCT -3’	This study	N/A
pGL3-DUOX1 AR neg cloning primers	This study	N/A

Fw- 5’- CCGAGCTCTTACGCGTCACCTGGACAGACTCTGTG -3’ Rv- 5’- TGCAGATCGCAGATCTCATGCCCCAACCAGAAGTG -3’		
pGL3- DUOX1_ARE_mut cloning Assembly PCR overlapped primers Fw- 5’- AGAAGTAATCTATGCTTTCTTGCACCGATGTTTAAGC -3’ Rv- 5’- GCATAGATTACTTCTAAGTCAAGGACCTTCTATAC -3’	This study	N/A
pA3F-AR cloning primers Fw- 5’- AATTGCCAGGATCCATGGAAGTGCAGTTAGGGC -3’ Rv- 5’- AAGGAAAAAAGCGGCCGCCTGGGTGTGGAAATAGATG -3’	This study	N/A
pA3F-ARΔDBD cloning Assembly PCR overlapped primers Fw- 5’- CATTGACTATTACTTTCCAGGGATGACTCTGGGAGC -3’ Rv- 5- GCTCCCAGAGTCATCCCTGGAAAGTAATAGTCAATG -3’	This study	N/A
pA3F-DNMT3A cloning primers Fw- 5’- CCGGAATTCATGCCCGCCATGCCCTCC -3’ Rv- 5- AAGGAAAAAAGCGGCCGCCACACACGCAAAATACTC -3’	This study	N/A
ChIP oligonucleotides		
(AR/ BRD4/ H3K27ac/ FOXA1)-DUOX1_pos binding ChIP primer set 1 (site 1) Fw- 5’- CCTCCTGAGTGGGTATAGAAGGT -3’ Rv- 5’- AGGGTGTAACAGCTGACTCC -3’	This study	N/A
(AR/ BRD4/ H3K27ac/ FOXA1)-DUOX1_pos binding ChIP primer set 2 (site 2) Fw- 5’- GCATCTATTGTTTGCTAGGCAC -3’ Rv- 5’- GCAAGAAAGCACAGATTGTTCC -3’	This study	N/A
AR-DUOX1_negative binding ChIP primers (NB site) Fw- 5’- CCCAACACCTGTCACTTGCT -3’ Rv- 5’- CCTCTTCCAGCTATGGGAGC -3’	This study	N/A
DNMTs-DUOX1_pos binding ChIP primer set 1 (site 1) Fw- 5’- AGAGGCGGAGGGTGGGAGAG -3’ Rv- 5’- GCCCCGCGTCACCCCGCCCT -3’	This study	N/A
DNMTs-DUOX1_pos binding ChIP primer set 2 (site 2) Fw- 5’- TCATCATGGCCCCAGACGGT -3’ Rv- 5’- GGAGATTCTGGGGCCTCAGT -3’	This study	N/A
AR-KLK2_pos binding ChIP primers (site 1) Fw- 5’- AGCAAACTTGTCCAGTC-3’ Rv- 5’- GTATCGCCTTCAGATCTAG -3’	This study	N/A
AR-UGT2B28_pos binding ChIP primers Fw- 5’- GGGTACTTGCAAGGTCATTAA -3’ Rv- 5’- CATAACTCCTTCAATCCAAAGT -3’	This study	N/A

Table S7. Plasmids generated and used in this study.

Recombinant Plamids	Source	Identifiers
pA3F (Empty vector)	Gift from Erle S Robertson (University of Pennsylvania),	PMID: 22438805
pEGFP-C1 (Empty vector)	Clontech laboratories, Inc	Cat No. 632470
pGIPZ-sh-Control	Gift from Erle S Robertson (University of Pennsylvania)	PMID: 38530845
pGIPZ-sh-DNMT3A	Gift from Erle S Robertson (University of Pennsylvania)	N/A
pA3F-DNMT3A	This study	N/A
pcDNA3/Myc-DNMT3B1	Addgene	Cat No. 35522
psPAX2	Addgene	Cat No. 12260
pMDG	Addgene	Cat No. 187440
pEGFP-C1-AR	Addgene	Cat No. 28235
pA3F-AR	This study	N/A
pGL3 Promoter Vector	Addgene	Cat No. 212939
pGL3 Promoter-DUOX1 reg-WT	This study	N/A
pGL3 Promoter-DUOX1 reg-Mut	This study	N/A
pGL3 Promoter-DUOX1 reg-Neg	This study	N/A
pA3F-ARΔDBD	This study	N/A
pSpCas9(BB)-2A-Puro (PX459) V2.0	Addgene	Cat No. 62988
PX459 V2.0-sgAR-1	This study	N/A
PX459 V2.0-sgAR-2	This study	N/A
PX459 V2.0-sgBRD4-1	This study	N/A
PX459 V2.0-sgBRD4-2	This study	N/A
PX459 V2.0-sgFOXA1-1	This study	N/A
pLX302_FOXA1-V5	Addgene	Cat No. 70090
pLVX-TetOne-Puro	Takara Bio Inc.	Cat No. 631849
pCMV3-DUOX1	Sino Biological, Inc.	Cat No. HG18937-UT
pLVX-TetOne-Puro-DUOX1	This study	N/A

Figure S1

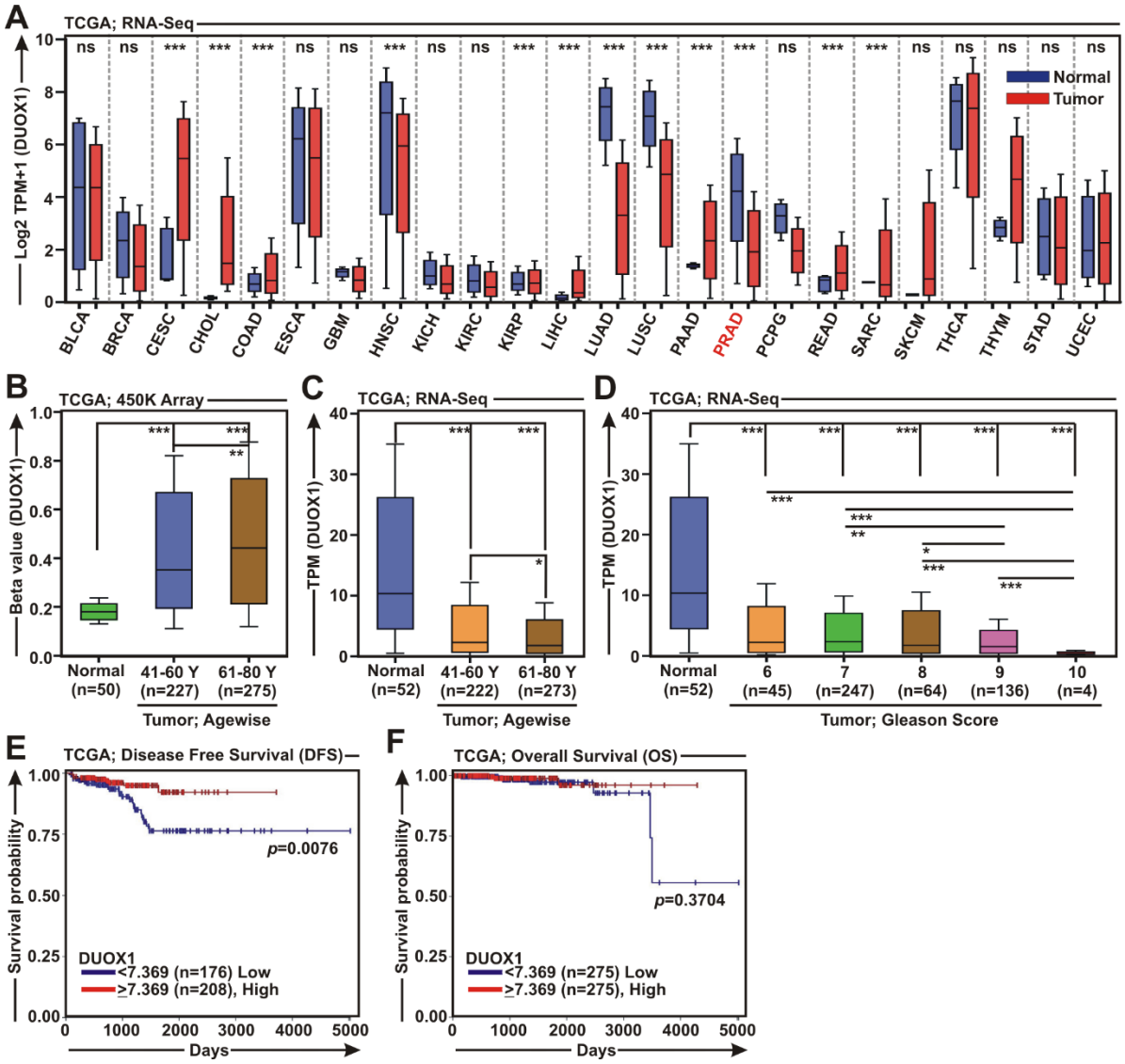

Figure S1. Promoter hypermethylation is associated with depletion of DUOX1 expression in TCGA-PRAD patient samples. **(A)** Box plots showing DUOX1 mRNA expression across 24 tumor types and matched normal tissues in the TCGA RNA-Seq dataset. **(B)** Box plot showing DUOX1 promoter methylation in normal and tumor samples across increasing patient age groups in the TCGA-PRAD 450K methylation dataset. **(C, D)** Box plots depicting DUOX1 expression in normal and tumor samples stratified by increasing (C) patient age and (D) Gleason score in the TCGA-PRAD RNA-Seq dataset. **(E, F)** Kaplan-Meier plots showing (E) disease-free survival (DFS) and (F) overall survival (OS) of patients stratified based on high versus low DUOX1 expression. Significant differences were shown (*$p < 0.05$; ** $p < 0.01$; *** $p < 0.001$; ns, not significant).

Figure S2

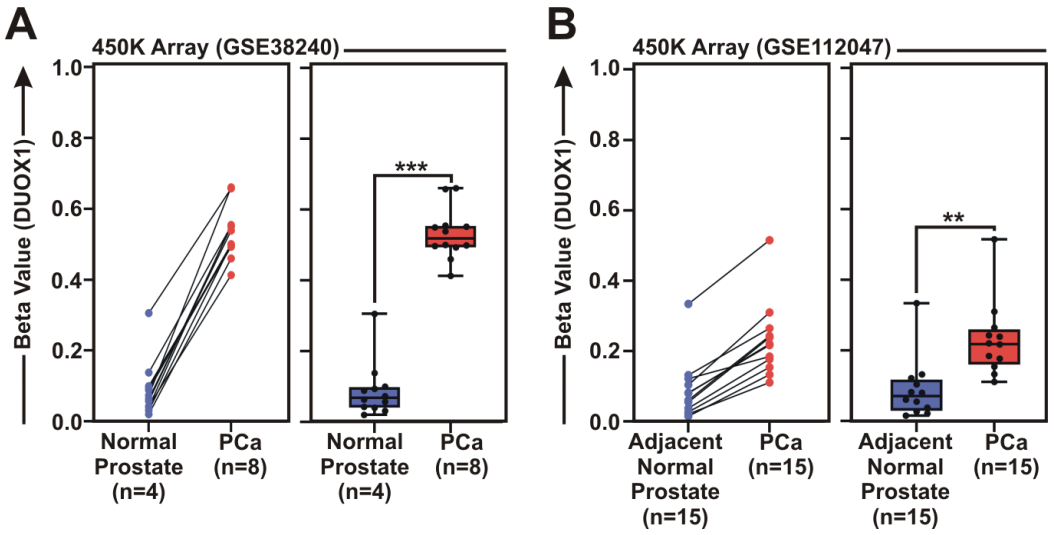

Figure S2. Reanalysis of 450K methylation array datasets in normal and PCa tissues. **(A, B)** Line and box plots showing DUOX1 promoter methylation in normal and primary PCa samples from two 450K methylation datasets (GSE38240 and GSE112047). Significant differences were shown (**$p < 0.01$; ***$p < 0.001$).

Figure S3

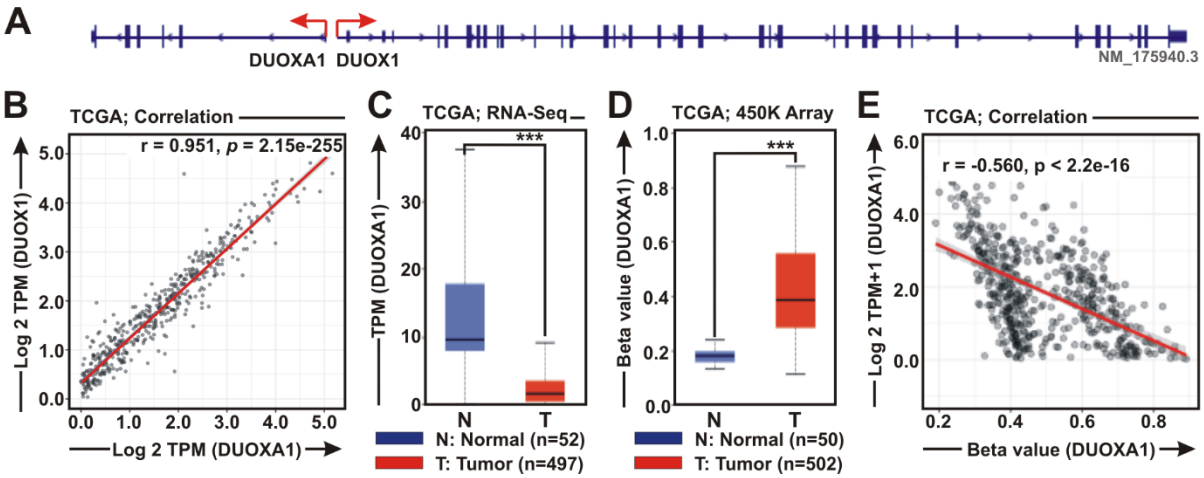

Figure S3. Expression of DUOX1 and its maturation factor DUOXA1 are coordinately regulated by promoter hypermethylation in PRAD. **(A)** Genome tracks illustrating the bidirectional organization of DUOX1 and DUOXA1 genes at chromosome 15q15–21. **(B)** Pearson correlation analysis between DUOX1 and DUOXA1 expressions in TCGA-PRAD samples. **(C)** RNA-Seq analysis showing DUOXA1 expression in normal and tumor samples from the TCGA-PRAD dataset. **(D)** 450K methylation array data showing DUOXA1 promoter methylation levels in normal and tumor samples from the TCGA-PRAD dataset. **(E)** Pearson correlation analysis between DUOXA1 promoter methylation and gene expression in the TCGA-PRAD dataset. Significant differences were shown (***$p < 0.001$).

Figure S4

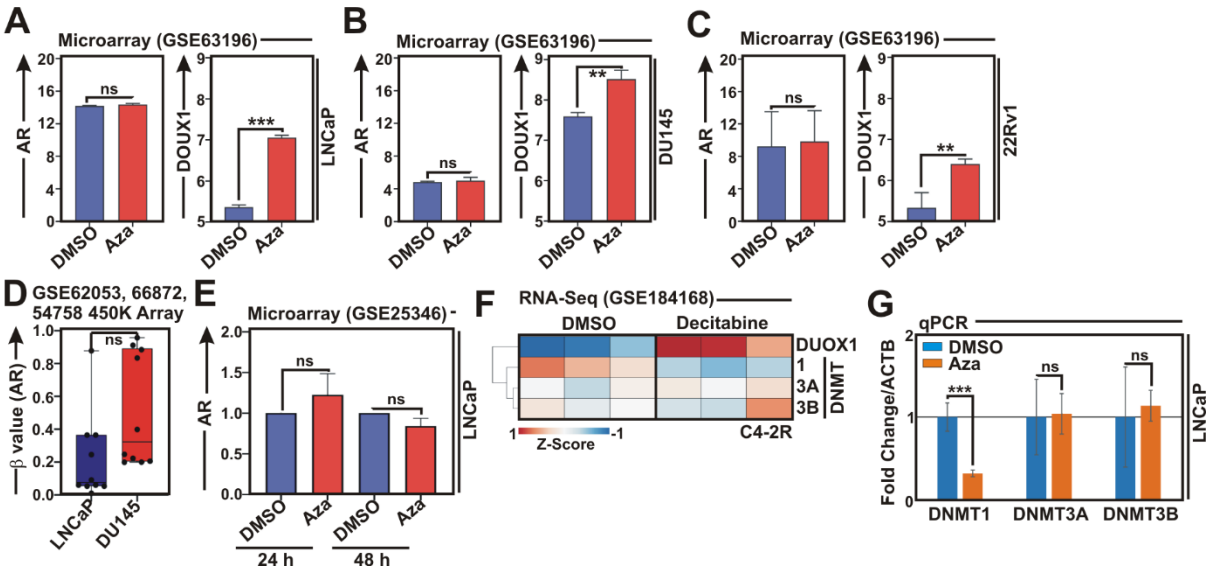

Figure S4. Demethylation restores DUOX1 expression in PCa cells. **(A-C)** Reanalysis of microarray data (GSE63196) showing AR and DUOX1 transcript levels in (A) LNCaP, (B) DU145, and (C) 22Rv1 cells following azacytidine (Aza) treatment. **(D)** 450K methyl array data (GSE62053, GSE66872 and GSE54758) showing AR promoter-methylation levels in LNCaP and DU145 cells. **(E)** Reanalysis of microarray data (GSE25346) showing AR expression in LNCaP cells upon Aza treatment for 24-48 h. **(F)** Heatmap showing relative mRNA expression of DUOX1 and DNMT members in RNA-Seq datasets of C4-2R cells with or without decitabine treatment. **(G)** qPCR showing mRNA expression profile of DNMT members in LNCaP cells with or without Aza treatment. Data were presented as the mean ± SD, n ≥ 3 biological replicates. Significant differences were shown (**$p < 0.01$; *** $p < 0.001$; ns, not significant).

Figure S5

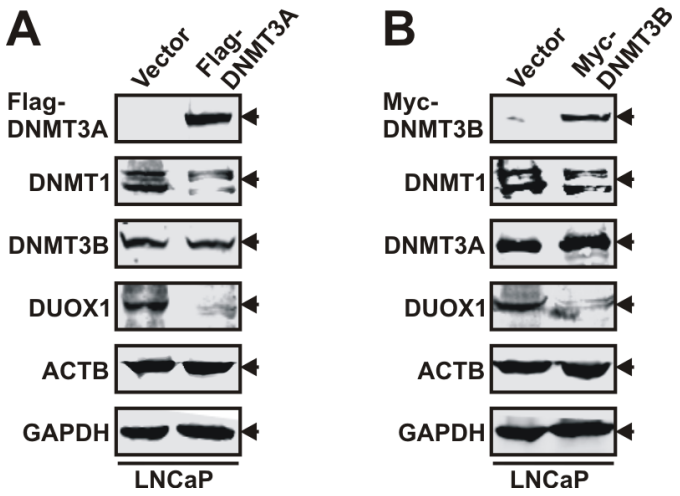

Figure S5. Ectopic expression of DNMT3A and DNMT3B reduces DUOX1 expression. **(A, B)** Western blot analyses of whole cell lysate from LNCaP cells transiently transfected with (A) flag-tagged DNMT3A or (B) myc-tagged DNMT3B expression plasmids.

Figure S6

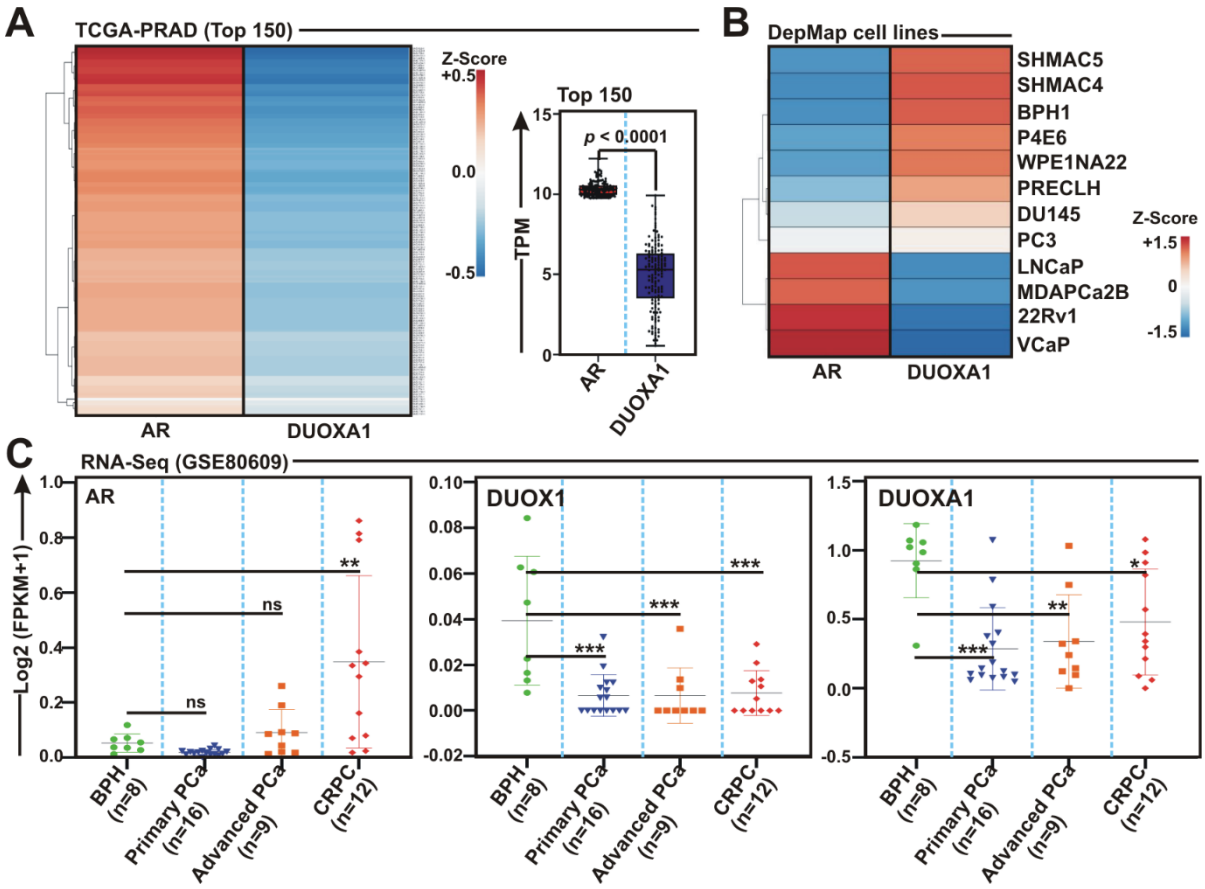

Figure S6. AR is negatively correlated with both DUOX1 and DUOXA1 expressions. (A) Heatmap showing RNA-Seq expression profiles of AR and DUOXA1 in primary PCa samples from the TCGA-PRAD dataset (top 150 samples with high AR expression). The corresponding box plot (right) illustrates the inverse correlation between AR and DUOXA1 expression. **(B)** Heatmap showing DUOXA1 expression in DepMap prostate cell lines (n = 12), stratified based on AR expression levels. **(C)** Dot plots of RNA-Seq data (GSE80609) from BPH, primary PCa, advanced PCa, and CRPC samples showing mRNA expression profiles of AR, DUOX1, and DUOXA1. Significant differences were shown (*$p < 0.05$; ** $p < 0.01$; *** $p < 0.001$; ns, not significant).

Figure S7

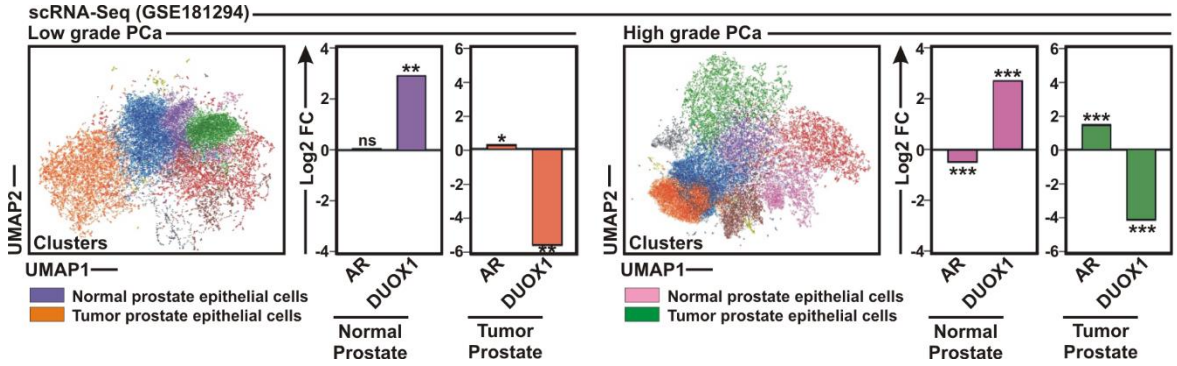

Figure S7. Single-cell RNA-seq analysis reveals an inverse correlation between AR and DUOX1 expression in prostate epithelial cells. UMAP (left) and bar (right) plots showing an inverse relationship between AR and DUOX1 expression in both normal and tumor epithelial cell populations derived from scRNA-Seq data (GSE181294) of two PCa samples. Significant differences were shown (*$p < 0.05$; ** $p < 0.01$; *** $p < 0.001$; ns, not significant).

Figure S8

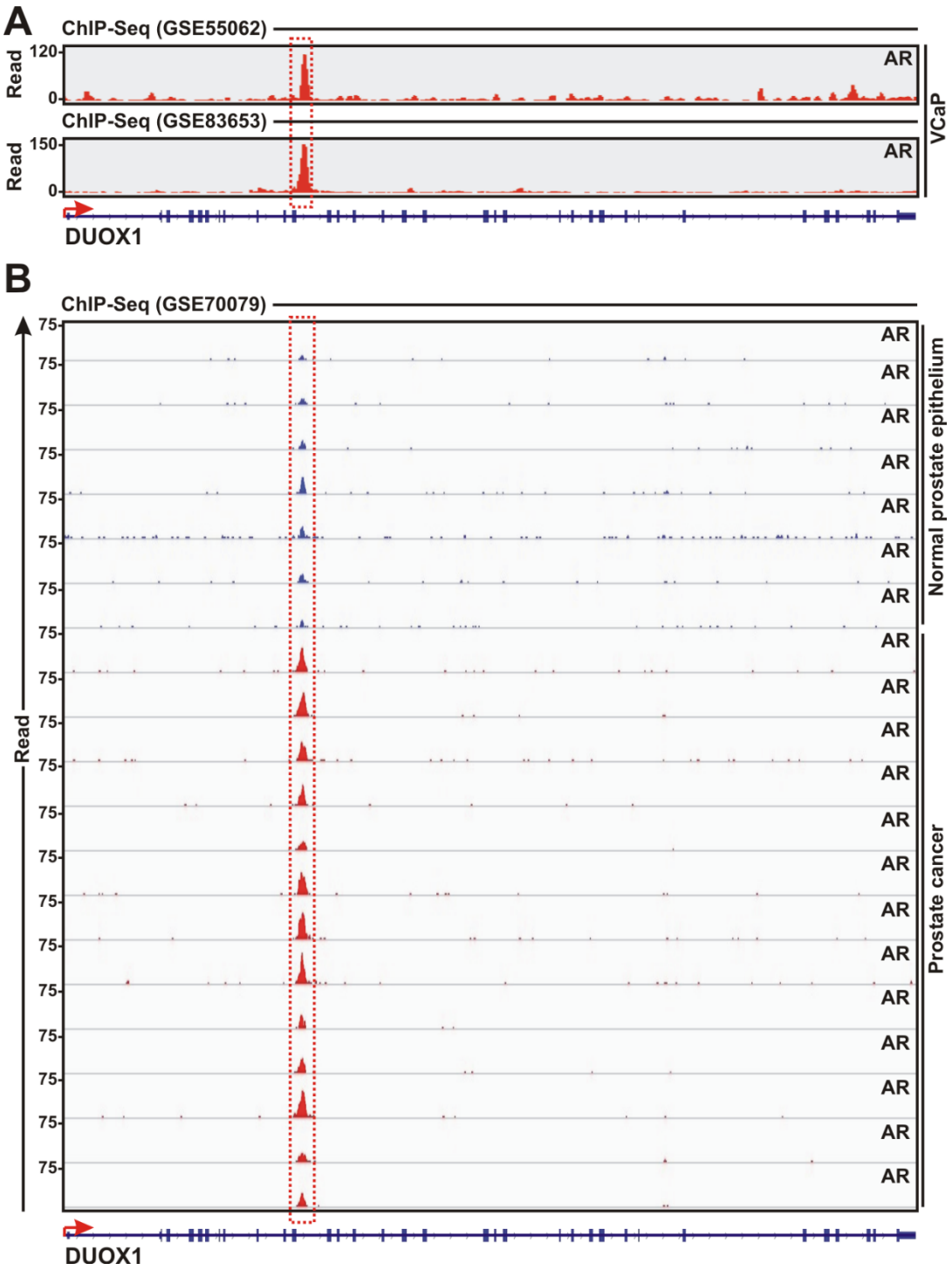

Figure S8. ChIP-Seq analysis reveals AR occupancy at the DUOX1 enhancer region. **(A)** ChIP-Seq tracks (GSE55062, GSE83653) in VCaP cells showing AR binding at an intragenic enhancer region within the DUOX1 locus. **(B)** ChIP-Seq tracks (GSE70079) showing increased AR occupancy at the DUOX1 locus in prostate cancer compared to normal prostate epithelial cells.

Figure S9

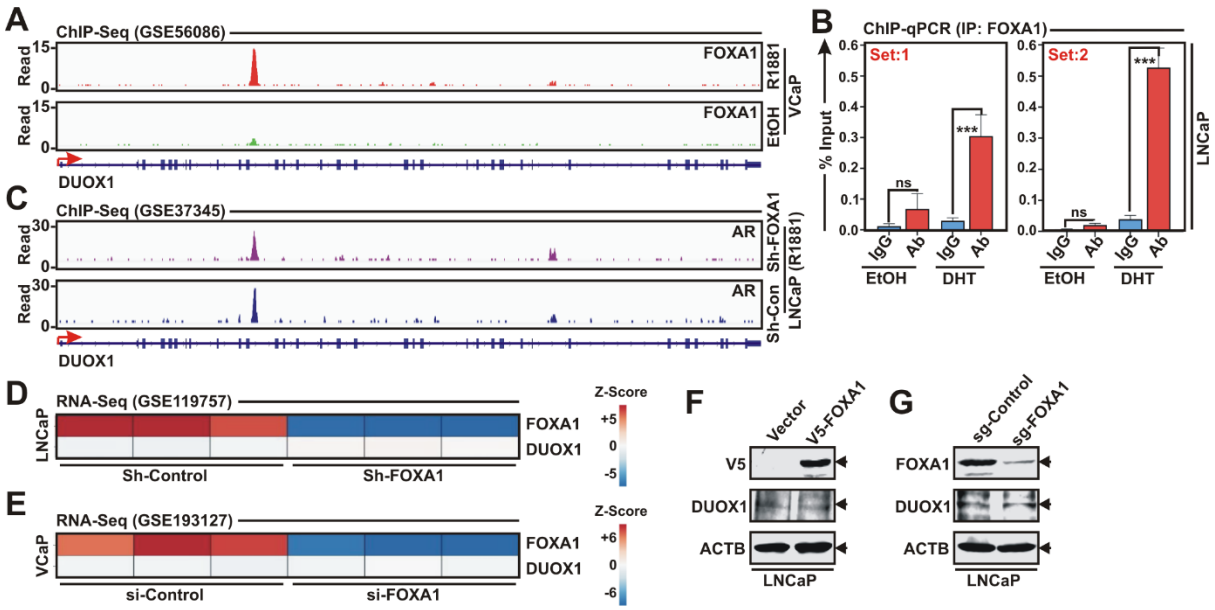

Figure S9. FOXA1 is dispensable for AR-mediated repression of DUOX1. **(A)** ChIP-Seq analysis (GSE56086) in VCaP cells showing FOXA1 recruitment to the DUOX1 enhancer region following androgen stimulation with R1881. **(B)** ChIP-qPCR analysis in LNCaP cells confirming androgen-induced FOXA1 binding to the DUOX1 enhancer using two primer sets (1 and 2). **(C)** ChIP-Seq analysis (GSE37345) showing no significant change in AR occupancy at the DUOX1 locus upon FOXA1 knockdown in R1881-treated LNCaP cells. **(D, E)** Heatmaps showing relative mRNA expression of FOXA1 and DUOX1 in RNA-Seq datasets of (D) LNCaP (GSE11975) and (E) VCaP (GSE193127) cells following FOXA1 knockdown. **(F, G)** WB analysis showing no significant change of DUOX1 expression following (F) FOXA1 overexpression or (G) FOXA1 knockout in LNCaP cells. ChIP-qPCR data were presented as the mean ± SD, n ≥ 3 biological replicates. Significant differences were shown (*** $p <$ 0.001; ns, not significant).

Figure S10

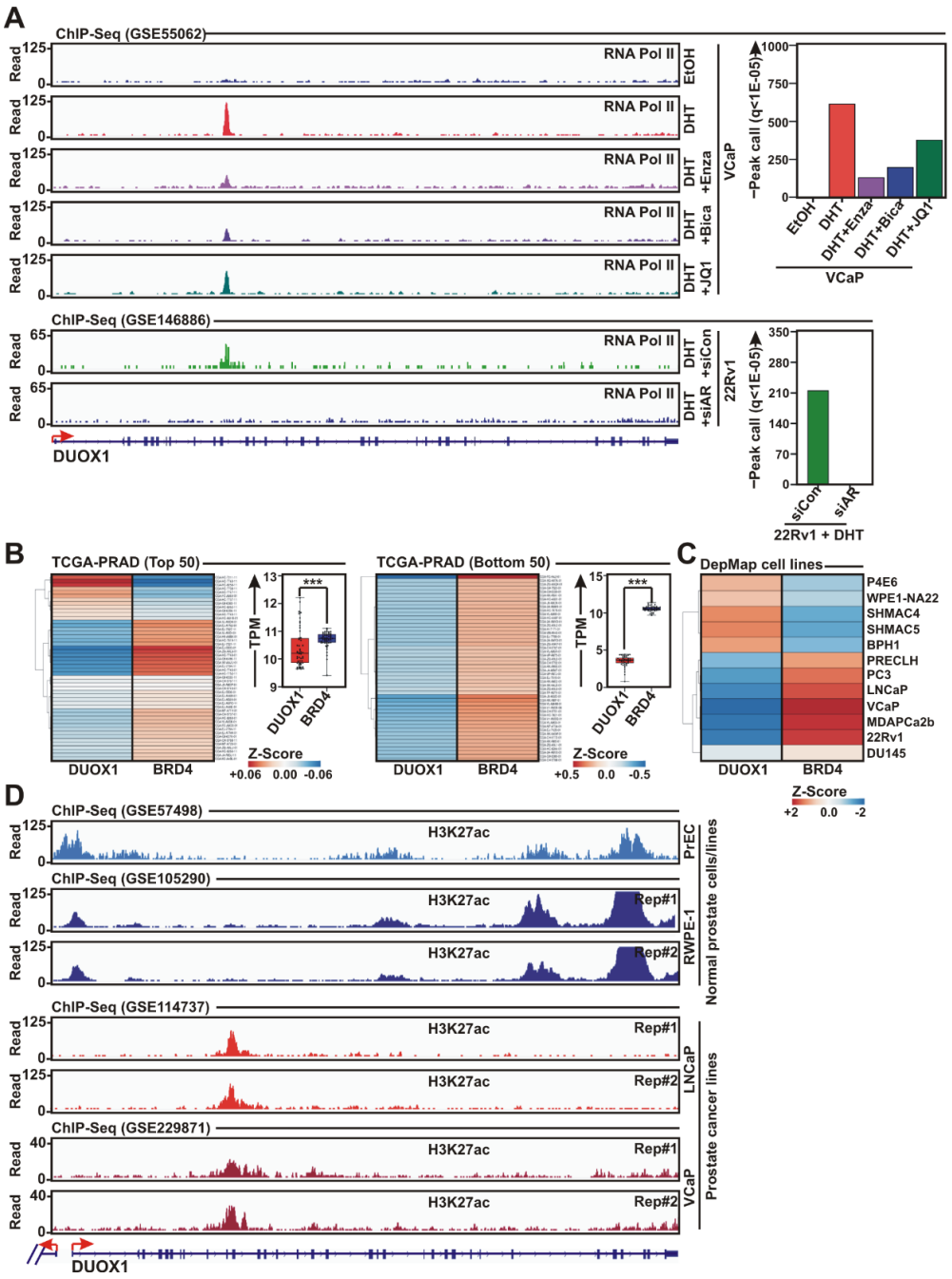

Figure S10. The AR-BRD4-H3K27ac axis negatively regulates DUOX1 expression in PCa. **(A)** ChIP-Seq tracks (right) showing enrichment of RNA polymerase II (RNA Pol II) at the DUOX1 intragenic enhancer region in VCaP (GSE55062) and 22Rv1 (GSE146886) cells under the indicated experimental conditions. Bar diagrams (right) showing peak calling of RNA Pol II enrichment. **(B)** Heatmap showing RNA-Seq expression profiles of DUOX1 and BRD4 in primary PCa samples from the TCGA-PRAD dataset (DUOX1 top and bottom 50 samples). The corresponding box plots (right) showing the inverse correlation between DUOX1 and BRD4 expression. **(C)** Heatmap showing relative expression of DUOX1 and BRD4 in DepMap prostate cell lines (n = 12). **(D)** ChIP-Seq datasets from normal/benign prostate (GSE57498, GSE105290) and PCa (GSE114737, GSE229871) cell lines indicating redistribution of H3K27ac signals from the DUOX1 promoter to the AR-bound enhancer region during PCa progression. Significant differences were shown (*** $p < 0.001$).

Figure S11

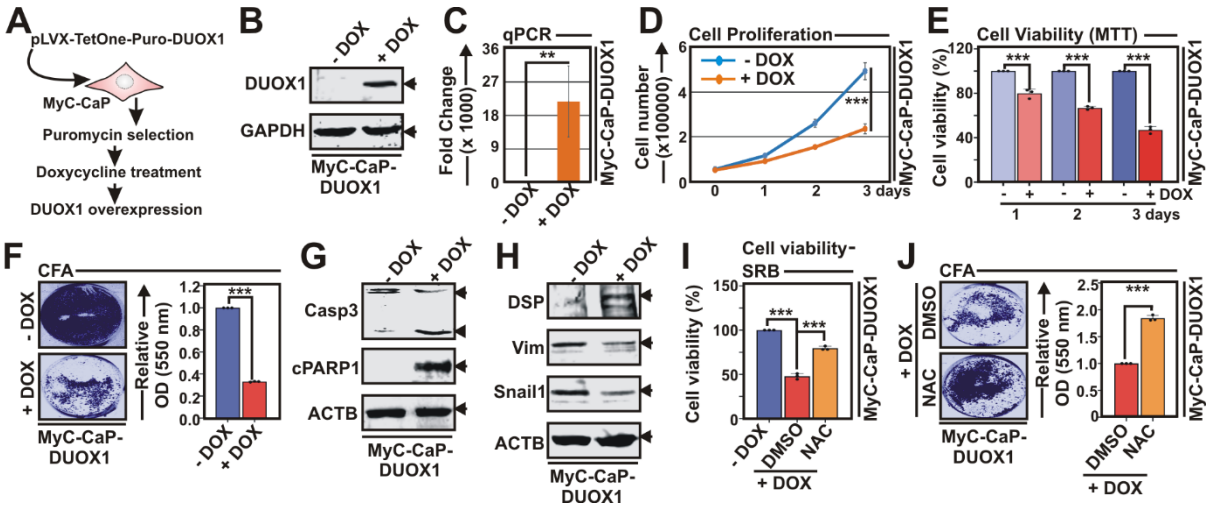

Figure S11. Ectopic expression of DUOX1 in mouse PCa line MyC-CaP induces cell death and anti-metastatic properties. **(A)** Schematic representation of the generation of a doxycycline (DOX)-inducible DUOX1 stable expression system in MyC-CaP cells (MyC-CaP-DUOX1). **(B)** WB analysis validating DUOX1 protein expression in DOX-treated MyC-CaP-DUOX1 cells. **(C)** qPCR analysis confirming inducible DUOX1 expression upon DOX treatment in MyC-CaP-DUOX1 cells. **(D)** Cell proliferation assay using the Trypan Blue exclusion method showing reduced growth of Myc-CaP-DUOX1 cells upon DOX induction over time (0-3 days). **(E)** MTT assay showing decreased cell viability of MyC-CaP-DUOX1 cells following DUOX1 induction over time (0–3 days). **(F)** Colony formation assay (CFA) demonstrating reduced clonogenic potential in DUOX1-expressing MyC-CaP cells upon DOX induction, with quantification of Crystal Violet staining at 550 nm (right panel). **(G)** WB analysis showing cleavage of apoptotic markers - Caspase-3 and PARP upon DUOX1 induction in MyC-CaP cells. **(H)** WB analysis showing differential expression of EMT markers upon DUOX1 induction in MyC-CaP cells. **(I)** Cell viability assays showing NAC-mediated rescue of cell death in DUOX1-expressing MyC-CaP cells using sulforhodamine B (SRB) assay. **(J)** CFA showing restoration of clonogenic potential in DUOX1-expressing MyC-CaP cells following NAC treatment, with quantification of Crystal Violet staining at 550 nm (right panel). Data were presented as the mean ± SD, n ≥ 3 biological replicates. Significant differences were shown (**$p < 0.01$; *** $p < 0.001$).

Figure S12

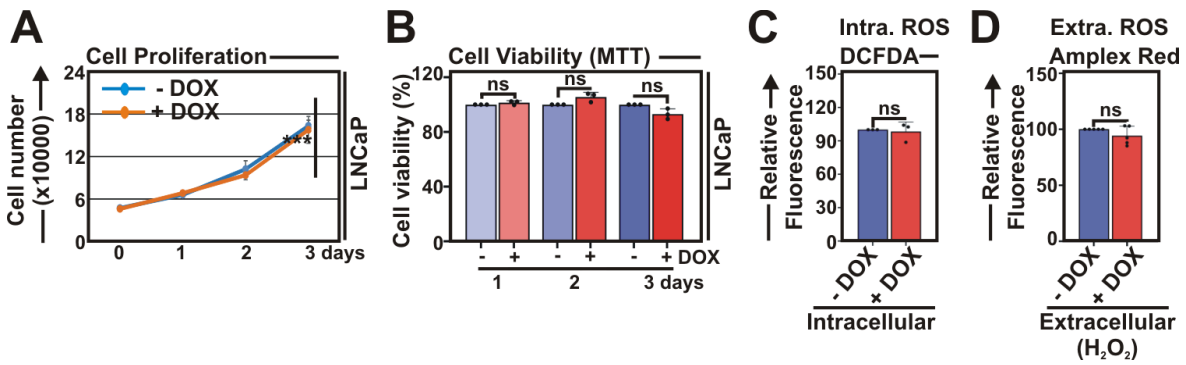

Figure S12. Doxycycline (DOX) treatment does not affect proliferation, viability or ROS production in parental LNCaP cells. **(A)** Trypan Blue exclusion assay showing no significant change in cell proliferation of LNCaP cells following treatment with 1 µg/mL DOX for 72 h. **(B)** MTT assay showing no significant change in cell viability under the same conditions. **(C, D)** DCFDA and Amplex Red assays showing no significant change in (C) intracellular ROS levels and (D) extracellular H_2O_2 production following 1 µg/ml DOX treatment for 48 h. Data were presented as the mean ± SD, n ≥ 3 biological replicates. Significant differences were shown (ns, not significant).

Figure S13

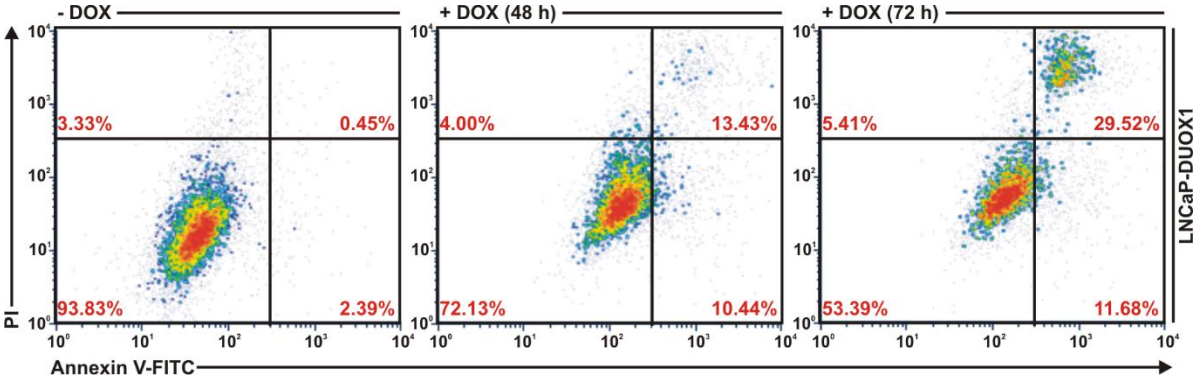

Figure S13. DUOX1 expression in LNCaP cells induces cell apoptosis. Annexin V/PI dual staining demonstrating increased apoptotic cell population following DUOX1 expression in LNCaP cells over time (0-72 h).

Figure S14

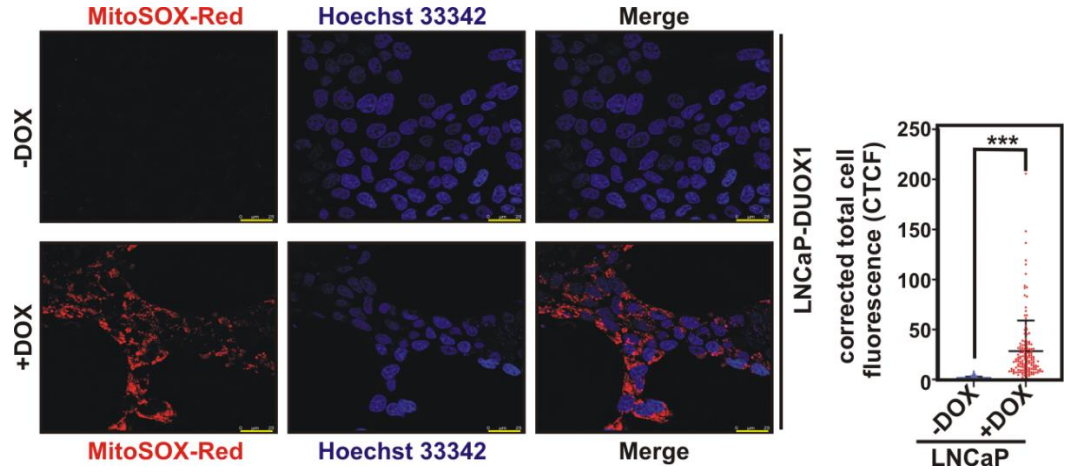

Figure S14. DUOX1 overexpression increases mitochondrial ROS in LNCaP cells. Representative fluorescence microscopy images showing mitochondrial superoxide levels measured by MitoSOX in LNCaP cells following DUOX1 induction. Nuclei were counterstained with Hoechst 33342. Scale bars, 25 µm. Dot plots of the same data (right) represent quantification of MitoSOX corrected total cell fluorescence (CTCF) per unit area, expressed as arbitrary units. Significant differences were shown (*** $p < 0.001$).

Figure S15

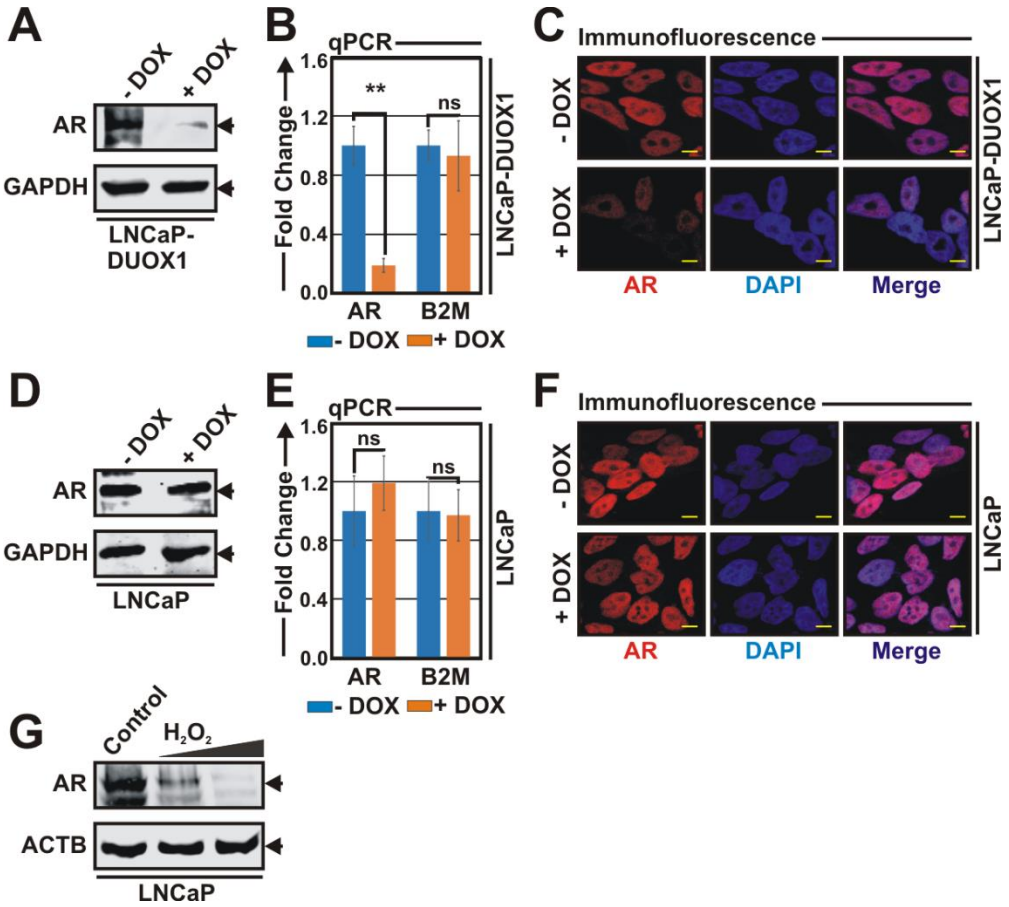

Figure S15. DUOX1 overexpression and H_2O_2 treatment reduce AR expression in LNCaP cells. **(A)** WB analysis showing reduced AR protein levels upon DUOX1 expression in LNCaP cells. **(B)** qPCR analysis showing decreased AR transcript levels following DUOX1 expression in LNCaP cells. **(C)** Immunofluorescence staining showing reduced AR (red) expression in DUOX1-expressing LNCaP cells. Nuclei were counterstained with DAPI (blue). Scale bars, 5 µm. **(D)** WB analysis showing no significant change in AR expression following doxycycline (DOX) treatment in parental LNCaP cells. **(E)** Immunofluorescence staining showing no significant change in AR (red) expression upon DOX treatment. Nuclei were counterstained with DAPI (blue). Scale bars, 5 µm. **(F)** WB analysis showing a dose-dependent decrease in AR expression following H_2O_2 treatment in LNCaP cells. Data were presented as the mean ± SD, n ≥ 3 biological replicates. Significant differences were shown (**$p < 0.01$; ns, not significant).

Figure S16

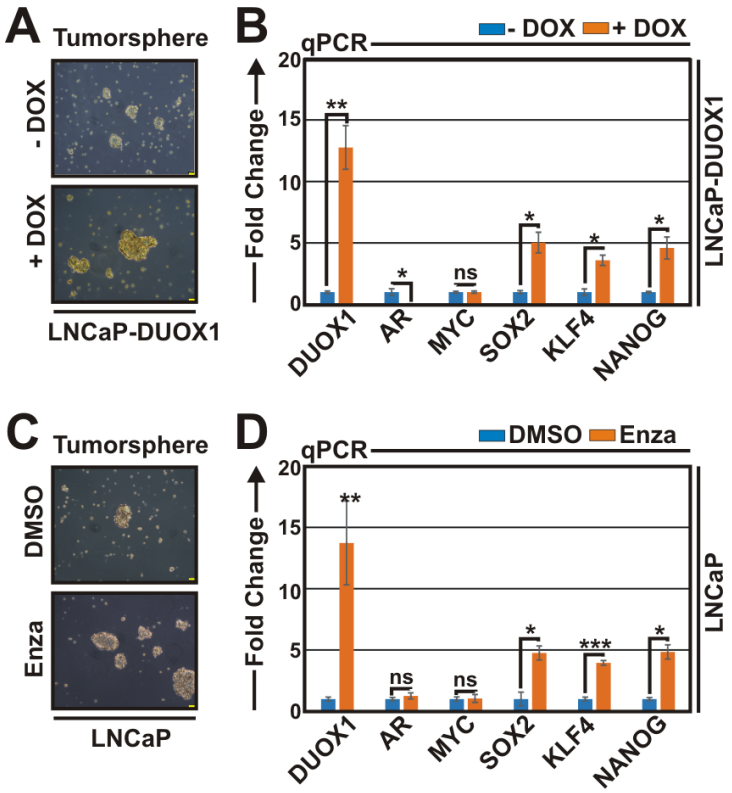

Figure S16. DUOX1-mediated AR downregulation promotes PCa stemness. **(A)** Representative phase-contrast images showing 3D tumor spheroids formed by LNCaP cells with or without DUOX1 expression following doxycycline (DOX) treatment. Scale bars, 50 µm. **(B)** qPCR analysis showing relative transcript levels of the indicated genes in LNCaP tumorospheres upon DUOX1 expression, as in (A). **(C)** Representative phase-contrast images showing 3D tumor spheroids formed by LNCaP cells with or without enzalutamide (Enza) treatment. Scale bars, 50 µm. **(D)** qPCR analysis showing relative transcript levels of the indicated genes in LNCaP tumorospheres following Enza treatment, as in (C). Data were presented as the mean ± SD, n ≥ 3 biological replicates. Significant differences were shown (* $p < 0.05$; ** $p < 0.01$; *** $p < 0.001$; ns, not significant).

Figure S17

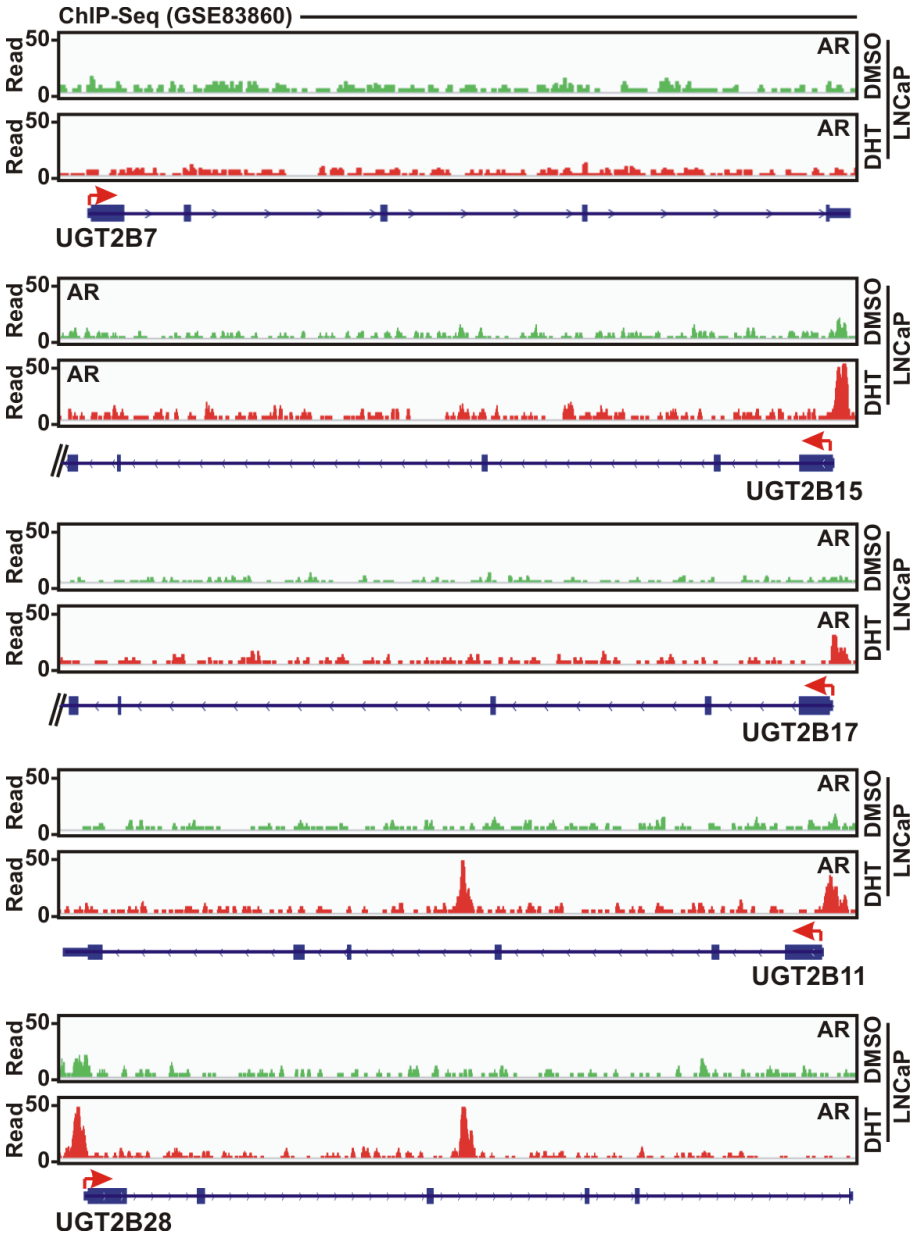

Figure S17. AR binds to the promoter regions of UGT2B family genes. ChIP-Seq tracks (GSE83860) in LNCaP cells showing AR enrichment at the promoter regions of UGT2B family members - UGT2B15, UGT2B17, UGT2B11, and UGT2B28, but not UGT2B7, following androgen stimulation with dihydrotestosterone (DHT).